The Astrophysical Journal, 639:L63–L66, 2006 March 10

NANODIAMOND AS A POSSIBLE CARRIER OF EXTENDED RED EMISSION

Huan-Cheng Chang and Kowa Chen
Institute of Atomic and Molecular Sciences, Academia Sinica, P.O. Box 23-166, Taipei 106, Taiwan; hcchang@po.iams.sinica.edu.tw
and
Sun Kwok
Institute of Astronomy and Astrophysics, Academia Sinica, P.O. Box 23-141, Taipei 106, Taiwan; and
Department of Physics and Astronomy, University of Calgary, Calgary, AB T2N 1N4, Canada;
kwok@asiaa.sinica.edu.tw
Received 2005 October 4; accepted 2006 January 26; published 2006 February 16

ABSTRACT

Diamond nanocrystals (size ~100 nm) emit bright luminescence at 600–800 nm when exposed to green and yellow photons. The photoluminescence, arising from excitation of the nitrogen-vacancy defect centers created by proton-beam irradiation and thermal annealing, closely resembles the extended red emission (ERE) bands observed in reflection nebulae and planetary nebulae. The central wavelength of the emission is ~700 nm, and it blueshifts to ~660 nm as the excitation wavelength decreases from 535 to 470 nm as the result of a combined excitation of two different detect centers [$(N\text{-}V)^-$ and $(N\text{-}V)^0$]. Our observations lend support to the suggestion that nanodiamond is a possible carrier for the ERE band.

Subject headings: dust, extinction — ISM: individual (NGC 2327) — planetary nebulae: individual (NGC 7027) — reflection nebulae — stars: AGB and post-AGB — stars: individual (HD 44179)

1. INTRODUCTION

Extended red emission (ERE) is a broad ($\Delta\lambda \sim 80$ nm), featureless emission band with a peak wavelength between 650 and 800 nm. ERE was first detected in the spectrum of HD 44179 (the Red Rectangle; Schmidt et al. 1980) and is commonly seen in reflection nebulae (Witt & Schild 1988; Witt & Boroson 1990). ERE has also been detected in dark nebulae, cirrus clouds, planetary nebulae, H II regions, the diffuse interstellar medium, and halos of galaxies (Smith & Witt 2002).

Since many solids emit visible luminescence when exposed to UV light, it is assumed that ERE is a photoluminescence process powered by far-UV photons. In the diffuse interstellar medium (ISM), approximately 4% of the energy absorbed by dust at wavelengths below 550 nm is emitted in the form of ERE, suggesting that the carrier of ERE must be a major component of the interstellar grains. It has been estimated that the intrinsic quantum yield of ERE is as high as 50% and that the ERE carrier can intercept 20% of the photons absorbed by interstellar dust in the 90–550 nm range (Smith & Witt 2002). This limits the chemical composition of the ERE carrier to a few abundant and highly depleted elements, such as C, Fe, Si, and Mg. Since metals do not photoluminesce, the remaining possibilities are C and Si, with carbonaceous materials being the most likely candidates.

Proposed carriers of the ERE include hydrogenated amorphous carbon (Duley 1985; Duley & Williams 1988; Witt & Schild 1988; Furton & Witt 1993; Seahra & Duley 1999), quenched carbonaceous composites (Sakata et al. 1992), C_{60} (Webster 1993), and silicon nanoparticles (SNPs; Witt et al. 1998; Ledoux et al. 1998). Crystalline SNPs with 1.5–5.0 nm diameters have been suggested to possess optical properties that satisfy the spectral and quantum efficiency requirements. Laboratory studies have shown that SNPs can have quantum efficiencies near 100% and absorption coefficients 10 times higher than average interstellar dust (Ledoux et al. 2001). While the observed quantum efficiency and the overall spectral characteristics of the ERE process are well matched by the SNP model (Smith & Witt 2002), recent experiments indicate that the silicon nanoparticles could lose their photoluminescence capability in environments where cosmic ion bombardment plays a relevant role (Baratta et al. 2004).

Diamond is a possible carrier for the ERE band (Duley 1988). The material is chemically robust, optically transparent, and capable of emitting luminescence from point defects. Among more than 500 point defects in diamond, nitrogen-vacancy (N-V) defect centers (see Table 1) have been closely examined for more than 30 years (Davies et al. 1992). The negatively charged nitrogen-vacancy center, denoted $(N\text{-}V)^-$ (Mita 1996), receives the most attention because of its structural simplicity, thermal stability, and photoluminescence brightness. The center absorbs strongly at ~560 nm and emits intense luminescence at ~700 nm (Davies & Hamer 1976), with a quantum yield close to unity at room temperature (Collins et al. 1983). To create these color centers, synthetic or natural diamond containing isolated substitutional nitrogen atoms is first damaged by high-energy (i.e., 2 MeV) electron- or ion-beam irradiation and subsequently annealed at high temperatures (i.e., 800°C). The annealing brings the irradiation-created vacancy to a site proximate to the nitrogen atom, forming an $(N\text{-}V)^-$ center. The high quantum efficiency of the photoluminescence has made possible the observation of a single $(N\text{-}V)^-$ center at room temperature (Gruber et al. 1997; Jelezko et al. 2001).

Several laboratory and astronomical observations support the suggestion that nitrogen-containing diamond is a possible carrier for the ERE band. First, nitrogen is the major impurity in natural, synthetic, and meteoritic diamonds (Russell et al. 1991). In the diffuse ISM, where diamond dust may exist, the N-V defect centers in the dust can easily be produced by cosmic ion bombardment and subsequent annealing to high temperatures by absorption of UV photons. Second, the UV emission spectrum of the exciting object (HD 44179) of the Red Rectangle, which is the strongest stellar source of ERE, shows extreme carbon richness (Sitko 1983). This reflection nebula also exhibits strong infrared emission bands at 3.3, 6.2, 7.7,

TABLE 1

PROPERTIES OF SOME VACANCY-RELATED DEFECT CENTERS IN DIAMOND

Defect Center	Point Group	ZPL (nm)	λ_{em} (nm)	τ (ns)	ϕ
V^0 (GR1)	T_d	741.2	898	2.55	0.014
$(N\text{-}V)^-$	C_{3v}	637.6	697	11.6	0.99
$(N\text{-}V)^0$	C_{3v}	575.4	600	...	...
N-V-N (H3)	C_{2v}	503.5	531	16	0.95
N_3+V (N3)	C_{3v}	415.4	445	41	0.29

NOTE.—Listed are aymmetry, zero-phonon lines (ZPL), emission maxima (λ_{em}), emission lifetimes (τ), and quantum efficiencies (ϕ) (Davies 1994 and references therein).

8.6, and 11.3 μm, characteristics of aromatic hydrocarbon compounds. Third, the carrier of ERE is likely to have condensed in the circumstellar environment of proto–planetary nebulae and planetary nebulae and been ejected into the ISM (Witt et al. 1998). The fact that the material can survive journeys through the ISM and be spread throughout the halo of the Galaxy suggests that it must be a compound of robust nature. Nanodiamonds clearly satisfy this requirement.

2. EXPERIMENT

Synthetic type Ib diamond powders (containing typically 100 parts per million [ppm] nitrogen atoms) with a nominal size of 100 nm were obtained from Element Six (USA). They were purified in strong oxidative acids (Huang & Chang 2004) and resuspended in deionized water before use. A thin diamond film was prepared by depositing an aliquot of the suspension on a silicon wafer and dried in air. The film was then irradiated by a 3 MeV proton beam from an NEC tandem accelerator (9SDH-2, National Electrostatics Corporation) at a dose of 5×10^{15} protons cm^{-2} (Hsu et al. 2004). Formation of the $(N\text{-}V)^-$ centers was facilitated by annealing the proton-treated diamond nanocrystals in vacuum at 800°C for 2 hr. Fluorescence images were obtained using a laser scanning confocal fluorescence microscope (C1, Nikon) equipped with a 100 W mercury vapor lamp. The corresponding spectra were acquired with a photonic multichannel spectral analyzer (C7473, Hamamatsu).

According to SRIM Monte Carlo simulations (Ziegler et al. 1985), the typical concentration of the $(N\text{-}V)^-$ centers produced by the 3 MeV proton beam irradiation was on the order of $\sim 10^7$ μm^{-3} (Yu et al. 2005). To vary this concentration and promote the formation of neutral nitrogen-vacancy defect centers [$(N\text{-}V)^0$ in Table 1], the annealing temperature was lowered to $T = 600$°C (Davies 1979), while all other experimental conditions were kept the same.

3. RESULTS

Figure 1*a* shows the bright-field image of the fluorescent nanodiamonds (FNDs) and their aggregates on a glass slide. Excitation of the FNDs annealed at $T = 800$°C with the yellow lines ($\lambda_{ex} = 510$–560 nm) from the Hg lamp produced intense red luminescence (Fig. 1*b*). A zero-phonon line (ZPL) corresponding to the $^3A \rightarrow {}^3E$ electronic transition (Jelezko et al. 2001) of the $(N\text{-}V)^-$ center was detected at 638 nm, accompanied with broad phonon sidebands spanning from 600 to 800 nm (Fig. 2*a*). Compared with the spectra obtained for single $(N\text{-}V)^-$ centers created by electron-beam irradiation in a millimeter-sized diamond crystal (Gruber et al. 1997), the ZPL observed in this spectrum is significantly weaker. Moreover,

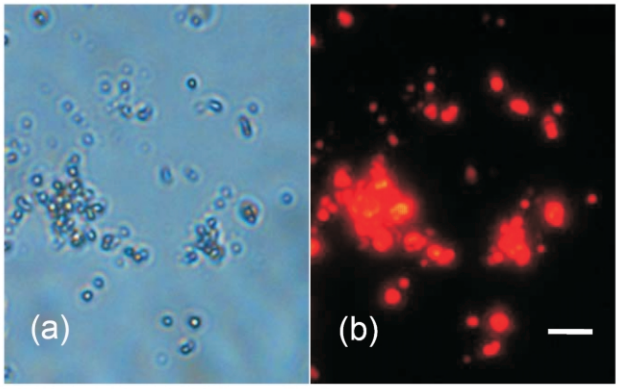

FIG. 1.—(*a*) Bright-field and (*b*) epifluorescence images of fluorescent nanodiamonds and their aggregates. The scale bar is 10 μm.

the phonon sidebands are broader and extend farther into the near-infrared (by ~20 nm), presumably because of sample heterogeneity. The emission spectrum is expected to be seen and broadened more extensively for smaller (a few nanometers) diamond particles as a consequence of the same effect.

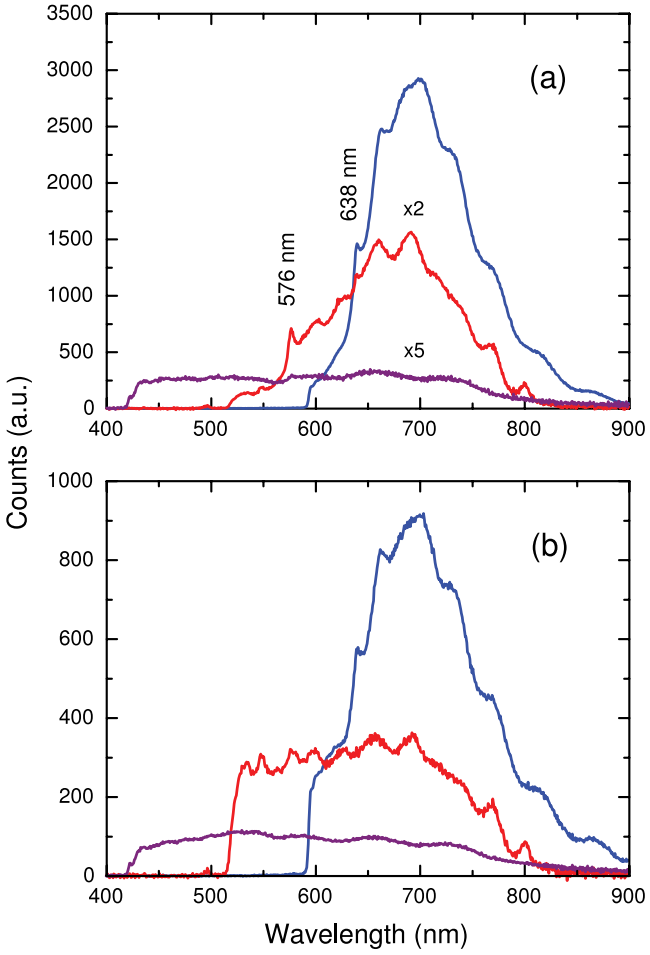

FIG. 2.—Photoluminescence spectra of proton-irradiated nanodiamonds annealed at (*a*) 800°C and (*b*) 600°C and excited with three different light sources: $\lambda_{ex} = 510$–560 nm (*top*, *blue*), 450–490 nm (*middle*, *red*), and 330–380 nm (*bottom*, *purple*). The corresponding emission was collected at $\lambda_{em} > 590$, 520, and 420 nm, respectively.

Excitation of the FND sample with the blue lines (λ_{ex} = 450–490 nm) from the Hg lamp results in a blueshift of the emission band and a roughly threefold decrease in total luminescence intensity (Fig. 2*a*). This intensity decreases further (~10-fold) upon excitation of the sample with the UV photons (λ_{ex} = 330–380 nm). The phenomenon is well understood as a result of the smooth decrease of the extinction coefficient of the $(N\text{-}V)^-$ absorption band from 560 nm to the UV region (Davies & Hamer 1976). In contrast to $(N\text{-}V)^-$, the $(N\text{-}V)^0$ defect center absorbs more strongly in the blue than in the yellow region (Davies 1979). The ZPL of this center appears as a weak feature at 576 nm, accompanied with a broad absorption phonon sideband peaking at 500 nm. From an excitation of the sample with the blue photons (450–490 nm), the residual $(N\text{-}V)^0$ defect centers that survive through the 800°C annealing can be clearly seen in the emission spectrum. The central wavelength of the emission shifts to 660 nm as the result of a combined excitation of these two types of detect centers [$(N\text{-}V)^-$ and $(N\text{-}V)^0$] (Fig. 2*a*). A similar λ_{ex}-dependent spectral change can be detected for the FNDs annealed at T = 600°C (Fig. 2*b*). We note that even though the thermal annealing was carried out at a significantly lower temperature for the latter sample (Fig. 2*b*), the spectral profiles of the emission produced by the yellow-line excitation are essentially the same for both samples in the extended red region.

Figure 3 shows a comparison between laboratory spectra and astronomical spectra for three different objects. The laboratory spectrum displayed in Figure 3*a* was acquired at λ_{ex} = 510–560 nm for FND annealed at 800°C, and it matches remarkably well with the ERE spectrum of the planetary nebula NGC 7027 (Furton & Witt 1990) in both band center and width. A similarly good match is achieved for the ERE band of the reflection nebula NGC 2327 (Witt 1988), where the laboratory spectrum was acquired with a combined excitation of λ_{ex} = 510–560 nm and λ_{ex} = 450–490 nm (Fig. 3*b*). It should be noted that the observed profile and peak wavelength of ERE vary from source to source, as well as within the same source, depending on the distance to the illuminating star. For example, the ERE spectrum acquired at 6″ south of the star HD 44179 in the Red Rectangle peaks at a shorter wavelength than those of NGC 7027 and NGC 2327 (Witt & Boroson 1990). One possible contributing factor to such variations could be the changing excitation radiation field. A satisfactory fit to the Red Rectangle 6″ south emission profile can indeed be achieved with the laboratory spectrum acquired at λ_{ex} = 450–490 nm only for the same FND sample (Fig. 3*c*). In particular, the sharp rise of the luminescence signal at ~560 nm in the ERE can be well reproduced by the laboratory spectrum.

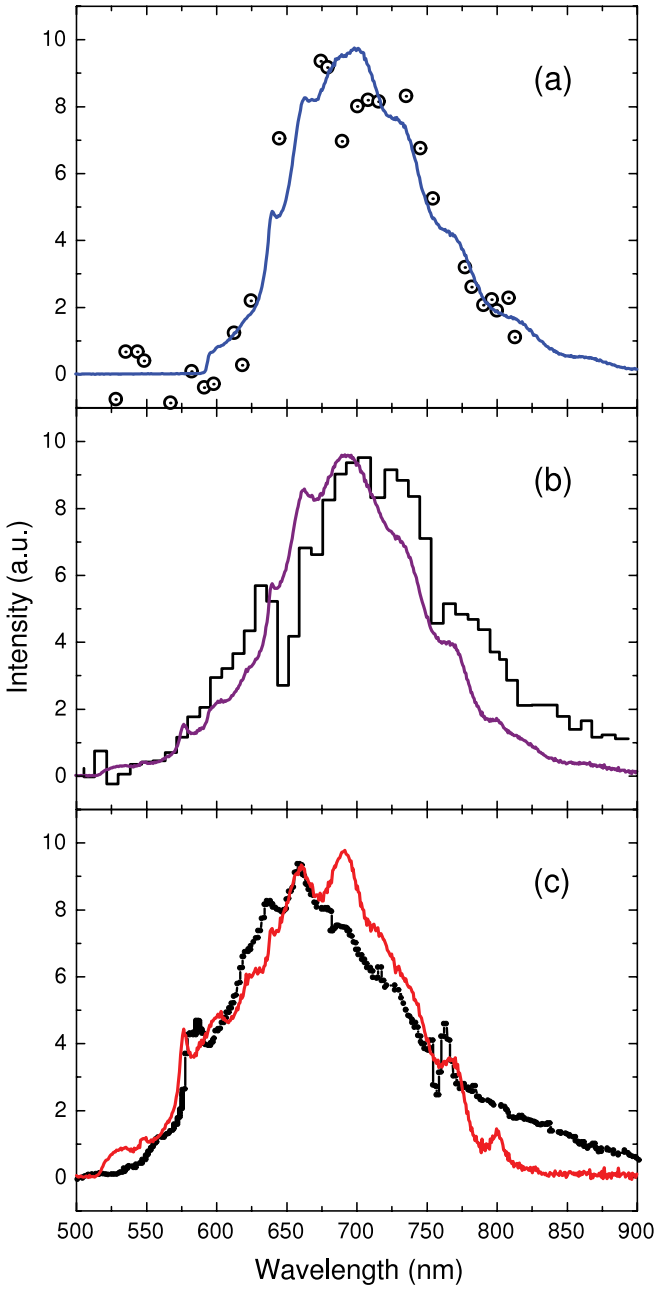

FIG. 3.—Comparison between laboratory spectra and astronomical spectra for three different objects: (*a*) NGC 7027 (*open circles*; Furton & Witt 1990), (*b*) NGC 2327 (*stepped horizontal lines*; Witt 1988), and (*c*) 6″ south of HD 44179 in the Red Rectangle (*dots with lines*; Witt & Boroson 1990). The laboratory spectra shown in (*a*)–(*c*) were acquired at (*a*) λ_{ex} = 510–560 nm, (*b*) λ_{ex} = 450–490 nm and λ_{ex} = 510–560 nm, and (*c*) λ_{ex} = 450–490 nm.

4. DISCUSSION

Many organic compounds are known to undergo photoluminescence. While it may be an extreme position to attribute the origin of ERE to biological material (Hoyle & Wickramasinghe 1999), there is almost no doubt that the ERE comes from a carbonaceous solid, as the presence of ERE is correlated with carbon-rich objects. A key to distinguish diamonds from other carbonaceous compounds may lie in the identification of the narrow features seen above the continuum (Schmidt et al. 1980; Van Winckel et al. 2002). An early attempt to make this identification has been carried out by Duley (1988), who pointed out the striking similarity between several sharp lines in the red luminescence spectra of brown diamonds (Pereira et al. 1986) and those observed in the luminescence spectra of the Red Rectangle. While the identification is still incomplete, the difference between laboratory and astronomical spectra appears to reflect a different defect distribution in the diamond-like material present in the Red Rectangle, since most ZPLs observed in the laboratory spectra are associated with lattice defects, impurities, or both. Indeed, a spread in line position of the ZPL at ~637 nm has been observed for four $(N\text{-}V)^-$ centers in detonation-synthesized nanodiamonds (Jelezko et al. 2001) containing high concentrations of impurities including H, N, and O atoms.

It has been noted experimentally that the $(N\text{-}V)^-$ centers are the dominant end products of annealing irradiation damage in

diamonds containing isolated substitutional nitrogen atoms (Davies & Hamer 1976). These defect centers are thermally stable up to 1000°C and emit strong photoluminescence at ~700 nm. This unique feature may explain why nearly all the ERE bands observed for the objects in reflection nebulae have a central wavelength in the range 650–700 nm (Witt & Boroson 1990). Although an interpretation of the band shift from object to object or even in different locations within the same object has been offered in terms of variations in size of the SNPs (Ledoux et al. 2001), such a band shift can be alternatively interpreted as a result of changes in the N-V center (due to different annealing temperatures) and in the excitation source (Fig. 2). Additional factors such as the defect composition (Table 1), the impurity content, and the degree of irradiation damage (Mita 1996; Brunetto et al. 2004) should also be taken into account. These factors clearly deserve close examination in future laboratory experiments. A study of the size effect on the emission profile and efficiency will also be pursued as we obtain new samples of nanodiamonds of smaller sizes.

Since the ERE is ubiquitous in the Galaxy, one may ask whether nanodiamonds qualify as a potential carrier from their expected interstellar abundance. We note that nanodiamonds have the highest abundance (1400 ppm) among all presolar grains in meteorites (Lewis et al. 1987). Although direct spectroscopic identification of diamond is difficult because of its lack of active infrared modes, surface vibrational modes of hydrogenated nanodiamonds have been detected in the spectra of two Herbig Ae/Be stars (Guillois et al. 1999). With respect to the Red Rectangle, the best example for ERE, the nebula is devoid of such diamond emission at 3.43 and 3.53 μm (Sheu et al. 2002). This observation, however, does not imply the absence of nanodiamonds in this nebula, because the presence of these CH stretching modes is limited to nanodiamonds of sizes at least 25 nm (Sheu et al. 2002), and smaller diamond particles such as those of meteoritic nanodiamonds (size ~3 nm) do not produce such emission (Jones et al. 2004). Furthermore, in order to exhibit these distinct CH stretching features, the nanodiamonds should be exposed to high H fluxes and strong UV fluxes so that high temperatures (up to 1000 K) can be reached to allow hydrogen etching, as well as hydrogenation, of the diamond surfaces to take place. In fact, because of the easy photoluminescience of nitrogen-containing nanodiamonds as demonstrated here, the ERE may be the strongest manifestation of nanodiamonds in the ISM.

The successful synthesis of diamonds under low-pressure conditions using chemical vapor deposition techniques has led to the realization that nanodiamonds can form in the circumstellar envelopes of carbon stars (Guillois et al. 1999; Sheu et al. 2002). The high concentration of H in the outflow allows the C atoms to aggregate into sp^3 hybridization (diamond) rather than the common sp^2 hybridization (graphite). A possible pathway of synthesis is growth from gas-phase carbon dimer (C_2), a molecule commonly observed in the photosphere of carbon stars. Vacancy-related defects can be produced by sputtering of the nanodiamond particles through grain-gas collisions, which are not dissimilar to the proton irradiation process used in our experiment.

5. CONCLUSION

Our laboratory observations of luminescence from diamond nanocrystals containing nitrogen-vacancy defects show a strong resemblance to the astronomical spectra of ERE. The circumstellar envelopes of carbon stars provide suitable conditions for the condensation of nanodiamonds and proton bombardment, leading to the formation of N-V defect centers. In the diffuse ISM, proton irradiation can be supplied by cosmic rays. Starlight, either direct or diffuse, excites the N-V centers, leading to photoluminescence. This scenario provides a consistent and reasonable explanation of the ERE phenomenon, suggesting that nanodiamonds could be a common ingredient of the solid-state component of the ISM.

We thank A. N. Witt for helpful discussions. This work is supported by grants to H.-C. C. and S. K. by Academia Sinica and the National Science Council of Taiwan. Support was also provided to S. K. by the Natural Sciences and Engineering Research Council of Canada. H.-C. C. thanks K.-M. Chen and Professor Y.-C. Yu at the Institute of Physics, Academia Sinica, for performing the proton-beam irradiation.

REFERENCES

Baratta, G. A., Strazzulla, G., Compagnini, G., & Longo, P. 2004, Appl. Surface Sci., 226, 57
Brunetto, R., Baratta, G. A., & Strazzulla, G. 2004, J. Appl. Phys., 96, 380
Collins, A. T., Thomaz, M. F., & Jorge, M. I. B. 1983, J. Phys. C, 16, 2177
Davies, G. 1979, J. Phys. C, 12, 2551
———, ed. 1994, Properties and Growth of Diamond (London: Inst. Electrical Eng.)
Davies, G., & Hamer, M. F. 1976, Proc. R. Soc. London A, 348, 285
Davies, G., Lawson, S. C., Collins, A. T., Mainwood, A., & Sharp, S. J. 1992, Phys. Rev. B, 46, 13157
Duley, W. W. 1985, MNRAS, 215, 259
———. 1988, Ap&SS, 150, 387
Duley, W. W., & Williams, D. A. 1988, MNRAS, 230, 1P
Furton, D. G., & Witt, A. N. 1990, ApJ, 364, L45
———. 1993, ApJ, 415, L51
Gruber, A., Dräbenstedt, A., Tietz, C., Fleury, L., Wrachtrup, J., & von Borczyskowski, C. 1997, Science, 276, 2012
Guillois, O., Ledoux, G., & Reynaud, C. 1999, ApJ, 521, L133
Hoyle, F., & Wickramasinghe, N. C. 1999, Ap&SS, 268, 321
Hsu, J.-Y., Yu, Y.-C., Liang, J.-H., Chen, K.-M., & Niu, H. 2004, Nucl. Instrum. Meth. Phys. Res. B, 219, 251
Huang, L.-C. L., & Chang, H.-C. 2004, Langmuir, 20, 5879
Jelezko, F., Tietz, C., Gruber, A., Popa, I., Nizovtsev, A., Kilin, S., & Wrachtrup, J. 2001, Single Mol., 2, 255
Jones, A. P., d'Hendecourt, L. B., Sheu, S.-Y., Chang, H.-C., Cheng, C.-L., & Hill, H. G. M. 2004, A&A, 416, 235
Ledoux, G., Guillois, O., Huisken, F., Kohn, B., Porterat, D., & Reynaud, C. 2001, A&A, 377, 707
Ledoux, G., et al. 1998, A&A, 333, L39
Lewis, R. S., Ming, T., Wacker, J. F., Anders, E., & Steel, E. 1987, Nature, 326, 160
Mita, Y. 1996, Phys. Rev. B, 53, 11360
Pereira, M. E., Jorge, M. I. B., & Thomaz, M. F. 1986, J. Phys. C, 19, 1009
Russell, S. S., Arden, J. W., & Pillinger, C. T. 1991, Science, 254, 1188
Sakata, A., Wada, S., Narisawa, T., Asano, Y., Iijima, Y., Onaka, T., & Tokunaga, A. T. 1992, ApJ, 393, L83
Schmidt, G. D., Cohen, M., & Margon, B. 1980, ApJ, 239, L133
Seahra, S. S., & Duley, W. W. 1999, ApJ, 520, 719
Sheu, S.-Y., Lee, I.-P., Lee, Y.-T., & Chang, H.-C. 2002, ApJ, 581, L55
Sitko, M. L. 1983, ApJ, 265, 848
Smith, T. L., & Witt, A. N. 2002, ApJ, 565, 304
Van Winckel, H., Cohen, M., & Gull, T. R. 2002, A&A, 390, 147
Webster, A. 1993, MNRAS, 264, L1
Witt, A. N. 1988, in Dust in the Universe, ed. M. E. Bailey & D. A. Williams (Cambridge: Cambridge Univ. Press), 1
Witt, A. N., & Boroson, T. D. 1990, ApJ, 355, 182
Witt, A. N., Gordon, K. D., & Furton, D. G. 1998, ApJ, 501, L111
Witt, A. N., & Schild, R. E. 1988, ApJ, 325, 837
Yu, S.-J., Kang, M.-W., Chang, H.-C., Chen, K.-M., & Yu, Y.-C. 2005, J. Am. Chem. Soc., 127, 17604
Ziegler, J. F., Biersack, J. P., & Littmark, U. 1985, The Stopping and Range of Ions in Solids (New York: Pergamon)